Central Core

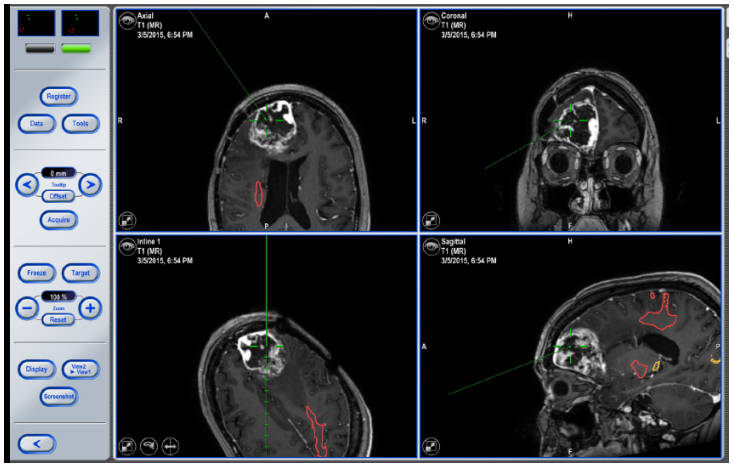

Enhancing Edge

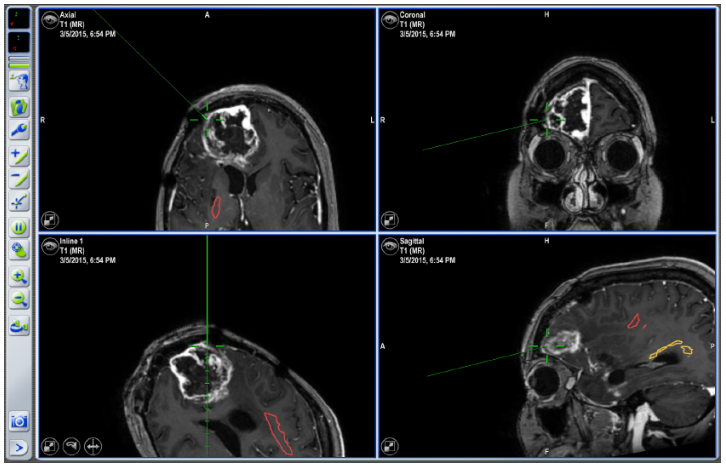

Infiltrated white matter (outside enhancement, within FLAIR)

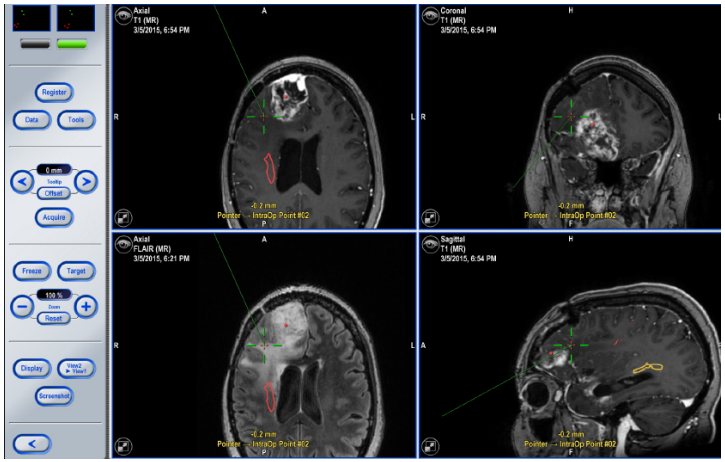

Supplementary Figure S1: Screen shots from the neuro-navigation illustrating where site-directed biopsies were taken from. Shown are screen shots taken from the neuro-navigation (BrainLAB system) illustrating locations of site-directed biopsies taken from the central core, enhancing edge, and infiltrated white matter of a representative bevacizumab-naïve recurrent glioblastoma.

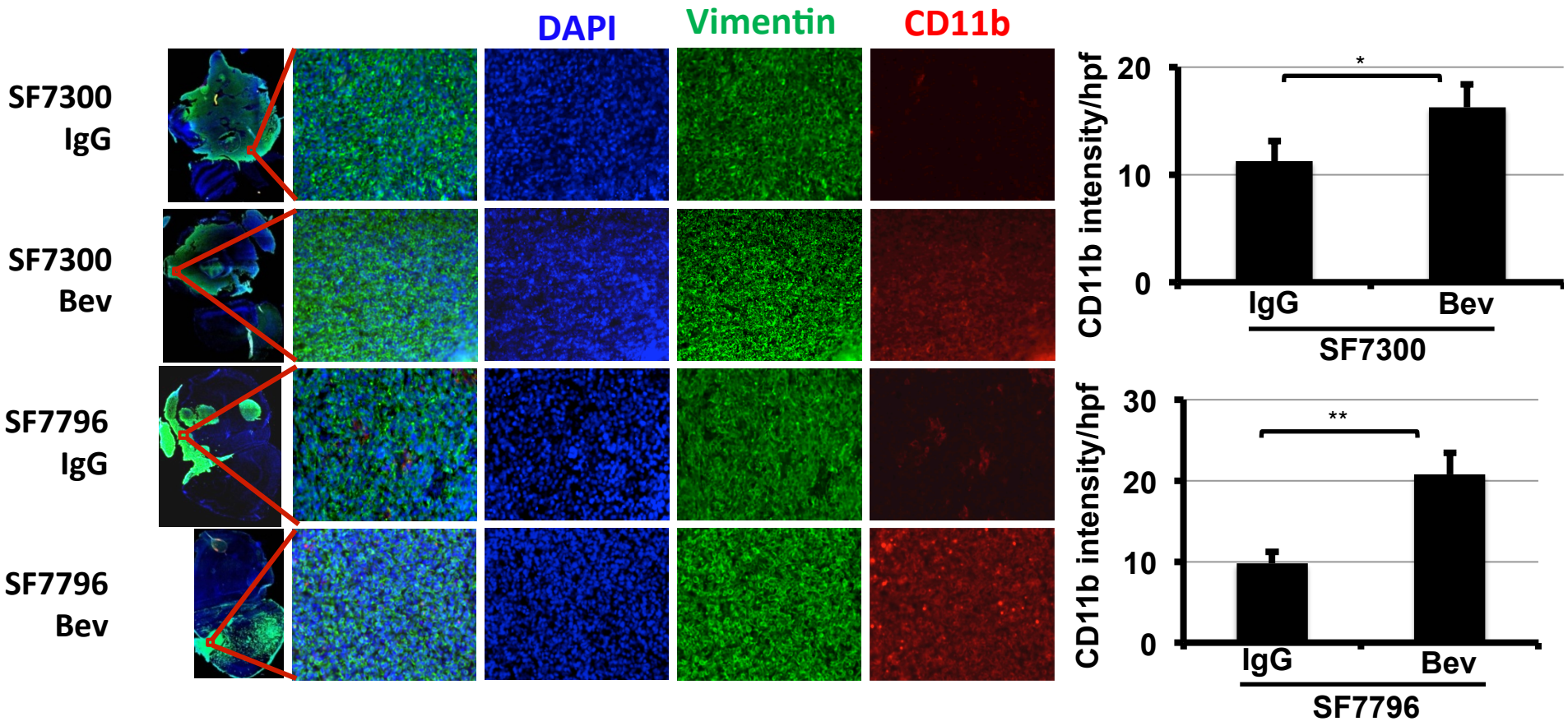

Supplementary Figure S2: Assessing tumor-associated macrophages in patient-derived bevacizumab sensitive versus resistant xenografts. Intracranial patient-derived xenografts which maintain the sensitivity (SF7300) or resistance (SF7796) of the patient glioblastoma they derived from were treated with IgG control antibody or bevacizumab (n=5/group). Resulting xenografts were stained for human vimentin (green) to visualize tumor cells, DAPI (blue) for nuclear staining, and CD11b (red) for macrophage staining. Image J analysis of red staining intensity revealed that bevacizumab increased TAMs significantly in both bevacizumab sensitive SF7300 (P=0.01) and bevacizumab-resistant SF7796 (P=0.002) xenografts (**Supplementary Fig. S1)**, but the increase in macrophages was significantly larger in bevacizumab-resistant SF7796 than bevacizumab-sensitive SF7300 xenografts (111% vs. 44%, p=0.01).

* *P*<0.05, ** *P*<0.01, *** *P*<0.001

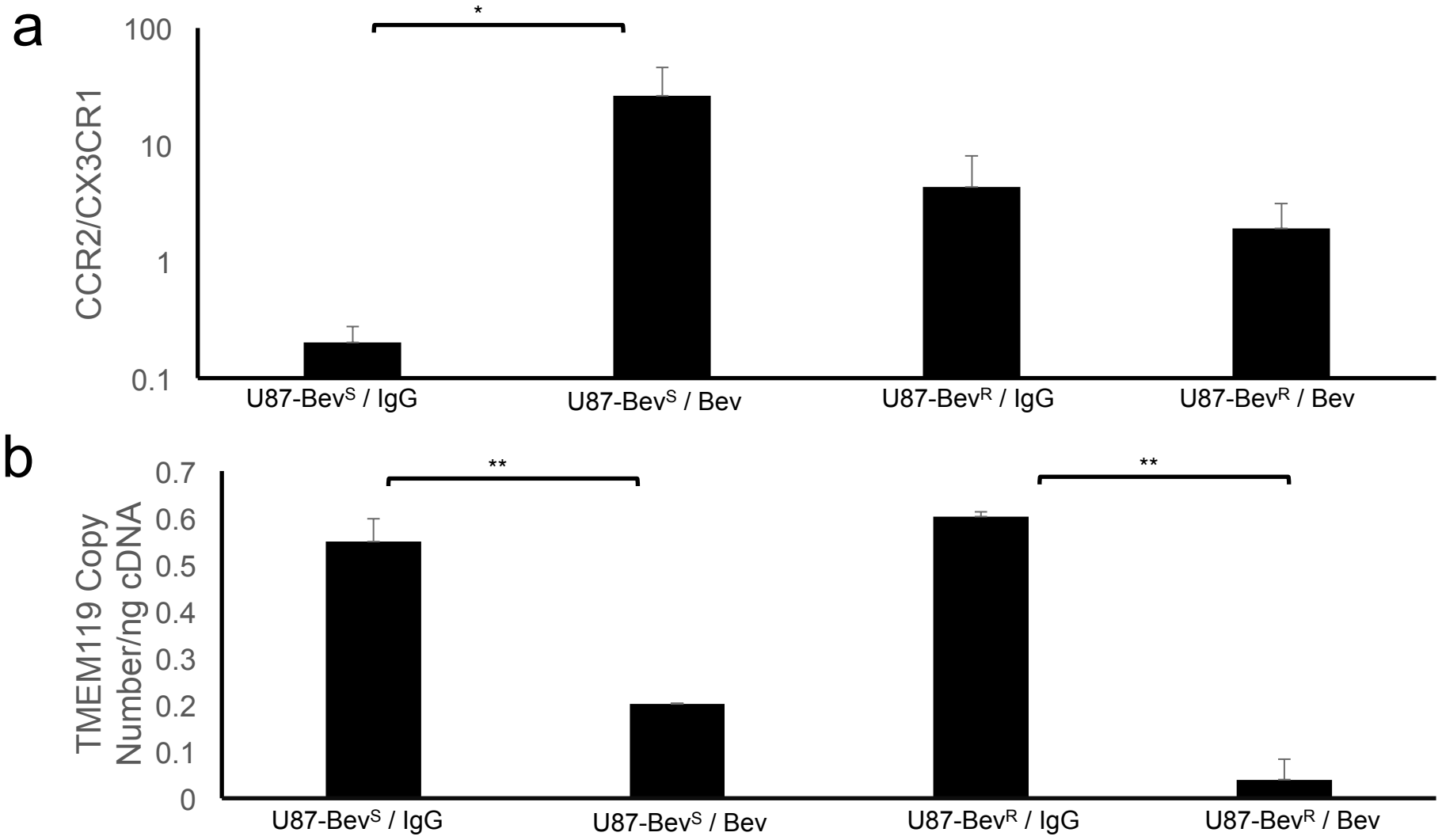

Supplementary Figure S3: Analyzing CD11b$^+$ cells for expression of macrophage versus microglia markers in bevacizumab-responsive versus resistant xenografts. CD11b$^+$ cells were isolated from intracranial U87-Bev^S and U87-Bev^R xenografts treated with IgG control antibody versus bevacizumab. qPCR was then used to analyze expression of (a) macrophage marker CCR2 and microglia marker CX3CR1, expressed as a ratio, which increased with bevacizumab treatment of U87-Bev^S (P=0.01) but not U87-Bev^R (P=0.6) xenografts; and (b) microglia marker TMEM119, expressed as copy number per ng of cDNA, which decreased with bevacizumab treatment of U87-Bev^S (P=0.001) and U87-Bev^R (P=0.002) xenografts. Error bars represent standard deviation (n=3/group).

* P<0.05, ** P<0.01, *** P<0.001

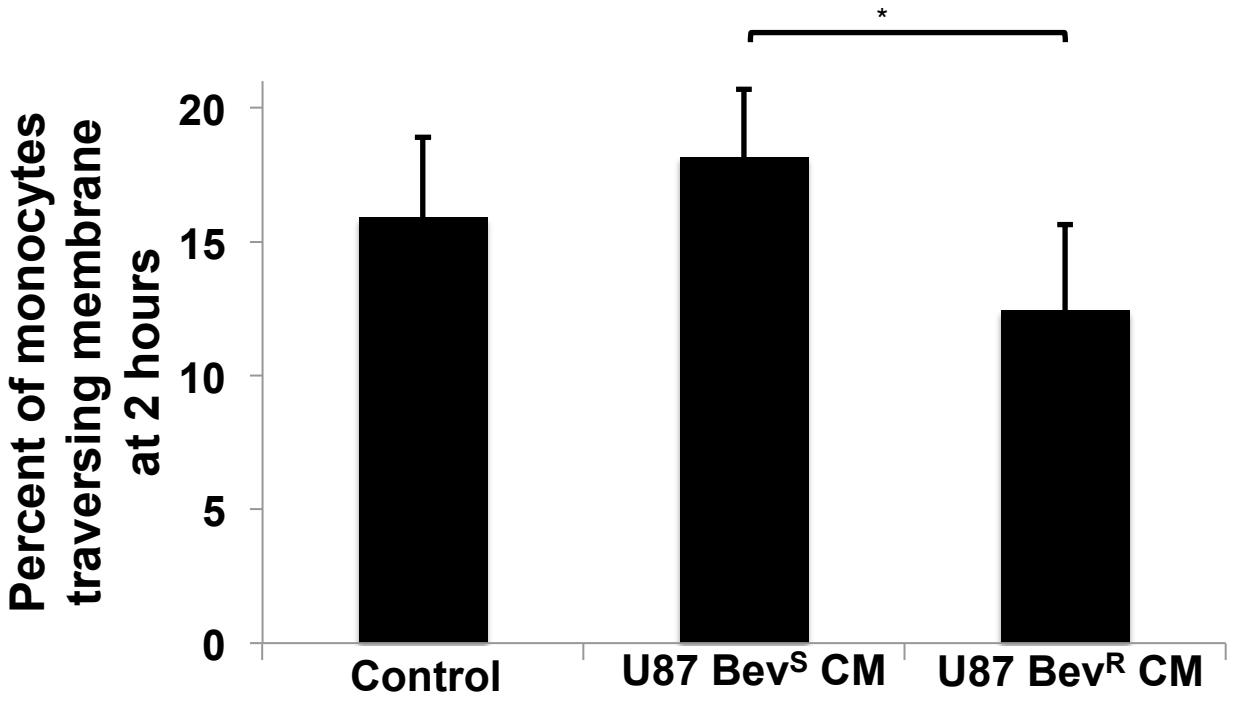

Supplementary Figure S4: Pre-treatment with U87-Bev^R conditioned media decreases chemotactic responsiveness. To assess the impact of tumor-conditioned media and macrophage migratory inhibitory factor (MIF) on monocyte chemotactic responsiveness, THP-1 monocytes were incubated for 20 hours in U87-Bev^R conditioned or U87-Bev^S conditioned media. The chemotactic response of THP-1 human monocytes to monocyte chemotactic protein-1 (MCP-1/CCL2) was reduced after pre-treatment with U87-Bev^R conditioned media compared to U87-Bev^S conditioned media (P =0.03) (n=4/group).

* P<0.05, ** P<0.01, *** P<0.001

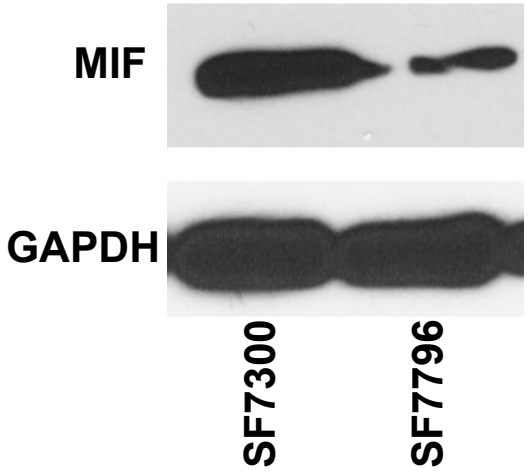

Supplementary Figure S5: Comparing MIF expression of bevacizumab-sensitive versus resistant patient-derived xenograft. Western blot revealed less MIF expression in lysates of intracranial xenografts derived from SF7796 (resistant) versus SF7300 (sensitive) patient-derived xenografts.

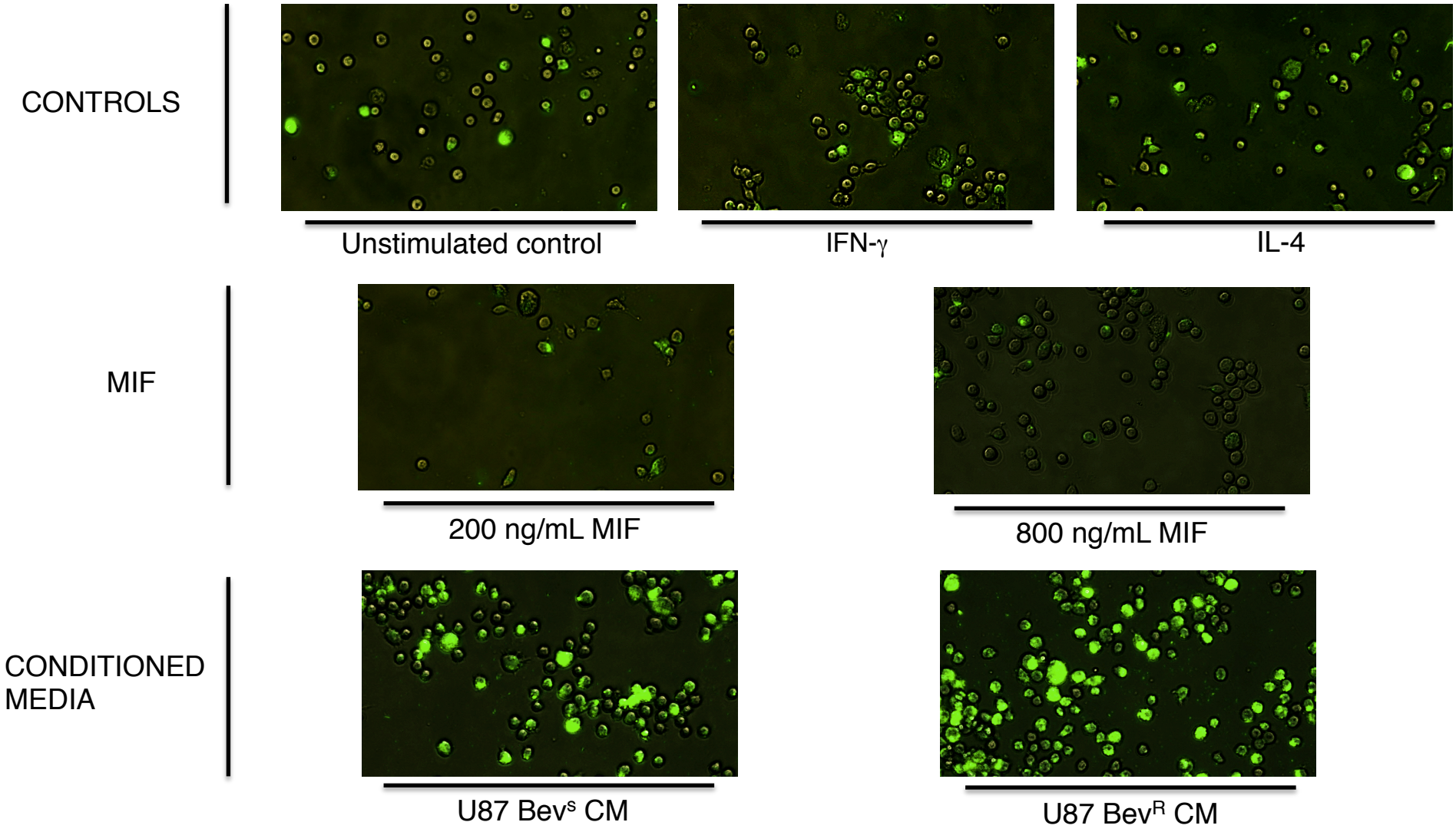

Supplementary Figure S6: Representative photos from phagocytosis assays. These representative photos are taken from all of the experimental groups in the phagocytosis assays depicted in **Fig. 2b**. In this assay, phagocytic activity of unstimulated macrophages derived from THP-1 monocytes and THP-1-derived macrophages treated with recombinant MIF, IFN-γ (M1 positive control), IL-4 (M2 positive control), or conditioned media (CM) was assessed via uptake of fluorescent heat-killed E. coli with subsequent measurement of the proportion of fluorescent cells. As shown in **Fig. 2b**, M1 polarized macrophages were less phagocytic whereas M2 polarized macrophages were more phagocytic relative to the unstimulated control. THP-1-derived macrophages treated with 800 ng/mL MIF were less phagocytic relative to control ($P=0.005$). Macrophages treated with CM from U87-Bev^R cells were more phagocytic than macrophages treated with U87-Bev^S CM ($P<0.05$) (n=6/group).

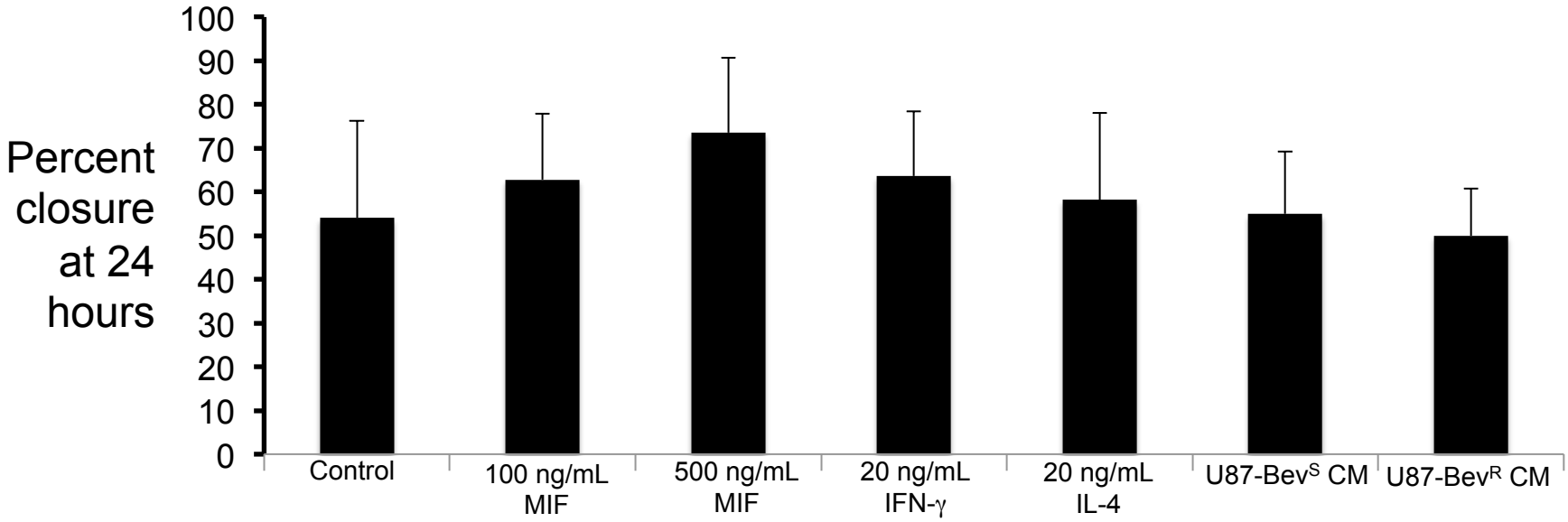

Supplementary Figure S7: Motility of tumor cells induced by sequential conditioned media from macrophages. Sequential conditioned media experiments were performed as illustrated in **Figure 3c**. Briefly, media from U87-Bev^R or U87-Bev^S cells or chemokines of varying concentration for controls were applied to THP-1-derived macrophages, and the media was then taken from those macrophages and applied to U87-MG cells. The motility of the U87-MG cells was then assessed using scratch assays. There was no significant difference in the motility of U87 cells grown in conditioned media from macrophages that were grown in 0 vs. 500 ng/mL MIF (P=0.3), 20 ng/mL IFN-γ (M1 positive control) vs. 20 ng/mL IL-4 (M2 positive control) (P =0.7), or conditioned media from U87-Bev^S vs. U87-Bev^R cells (P=0.6).

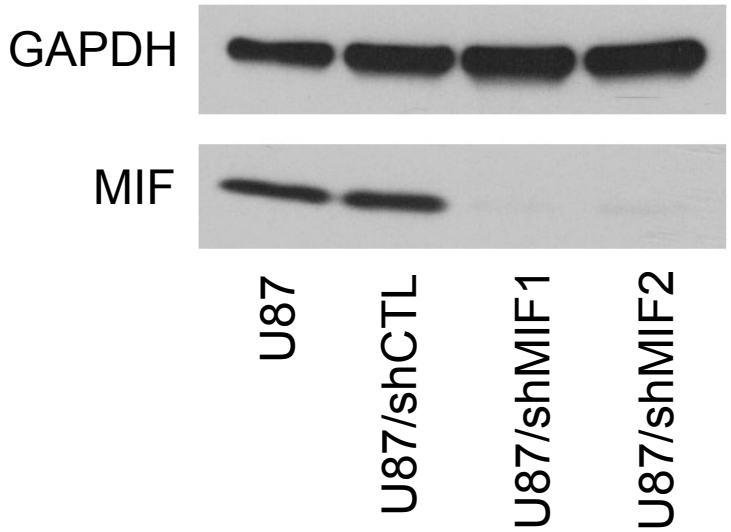

Supplementary Figure S8: Confirmation of MIF knockdown. Knockdown of MIF in U87 glioma cells transduced using a lentiviral MIF shRNA vector was confirmed via Western blot. Compared to normal U87 cells and U87 cells transduced with a non-specific shRNA construct (U87/shCTL), the average percent knockdown of MIF in U87 cells (assayed by band densitometry performed using ImageJ software) transduced with two different sequences of MIF-targeted shRNA (U87/shMIF1 and U87/shMIF2) when normalized to GAPDH was 91.1% and 98.9%, respectively.

U87/shCTL

U87/shMIF1

Supplementary Figure S9: Differential size and vascularity of MIF knockdown xenografts relative to control xenografts appreciated on gross visualization after brain explantation. Four weeks after implantation, explanted brains revealed that U87/shMIF tumors were grossly larger and more pink or yellow (suggesting greater vascularity) than U87/shCTL tumors, which were smaller and more pale.

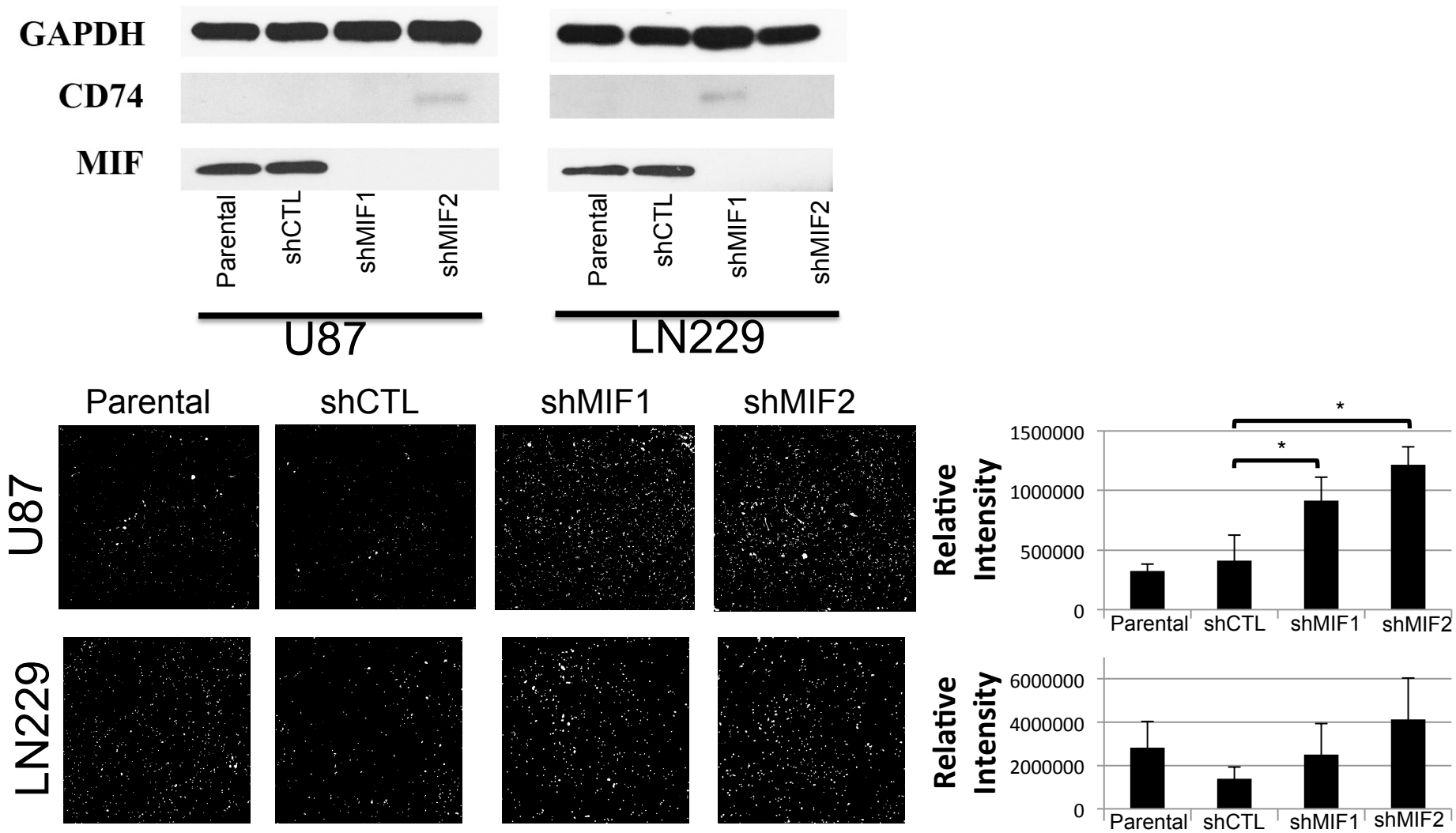

Supplementary Figure S10: Transduction with MIF shRNA increases or does not affect invasiveness in U87 and LN229 glioblastoma cells. Knockdown of MIF in U87 and LN229 glioma cells transduced using a lentiviral vector harboring two different MIF-targeted shRNAs (shMIF1 and shMIF2) relative to parental cells and cells transduced using a lentiviral vector harboring shRNA targeting control sequence (shCTL) were confirmed via Western blot. Matrigel chamber invasion assays revealed that, compared to parental cells and shCTL-transduced cells, U87/shMIF1 and U87/shMIF2 were more invasive (P=0.02 and 0.01, respectively), while LN229/shMIF1 and LN229/shMIF2 exhibited no change in invasiveness (P=0.8 and 0.4, respectively).The western blot also did not reveal much expression of MIF receptor CD74 in U87 and LN229.

* $P<0.05$, ** $P<0.01$, *** $P<0.001$

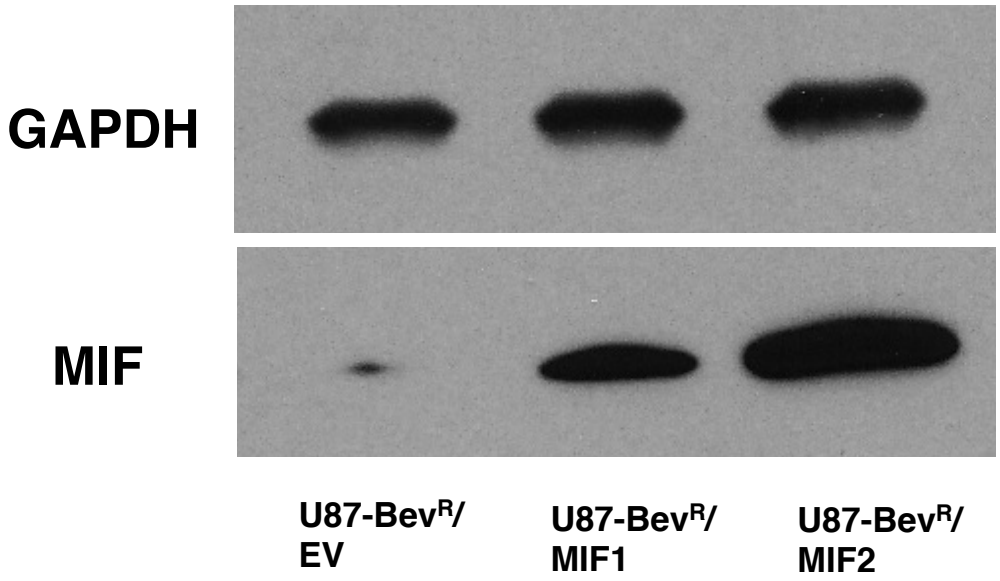

Supplementary Figure S11: Confirmation of MIF overexpression in transduced clones. Compared to U87-Bev^{R} cells transduced with empty vector (U87-Bev^{R}/EV), U87-Bev^{R} cells transduced with virus containing drug resistance gene and the human MIF cDNA followed by clonal selection to isolate two drug-resistant clones (U87-Bev^{R}/MIF1 and U87-Bev^{R}/MIF2) exhibited increased MIF expression.

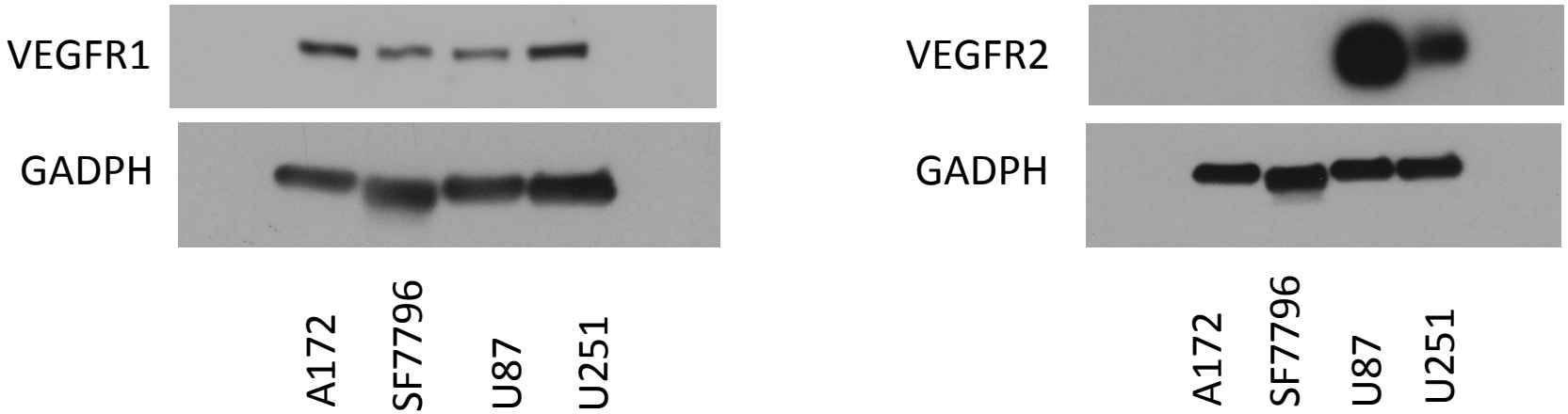

Supplementary Figure S12: Levels of VEGFR1 and VEGFR2 in four different glioma cell lines. All glioma cell lines expressed high amounts of VEGFR1, however only U87 and U251 cells expressed high levels of VEGFR2.

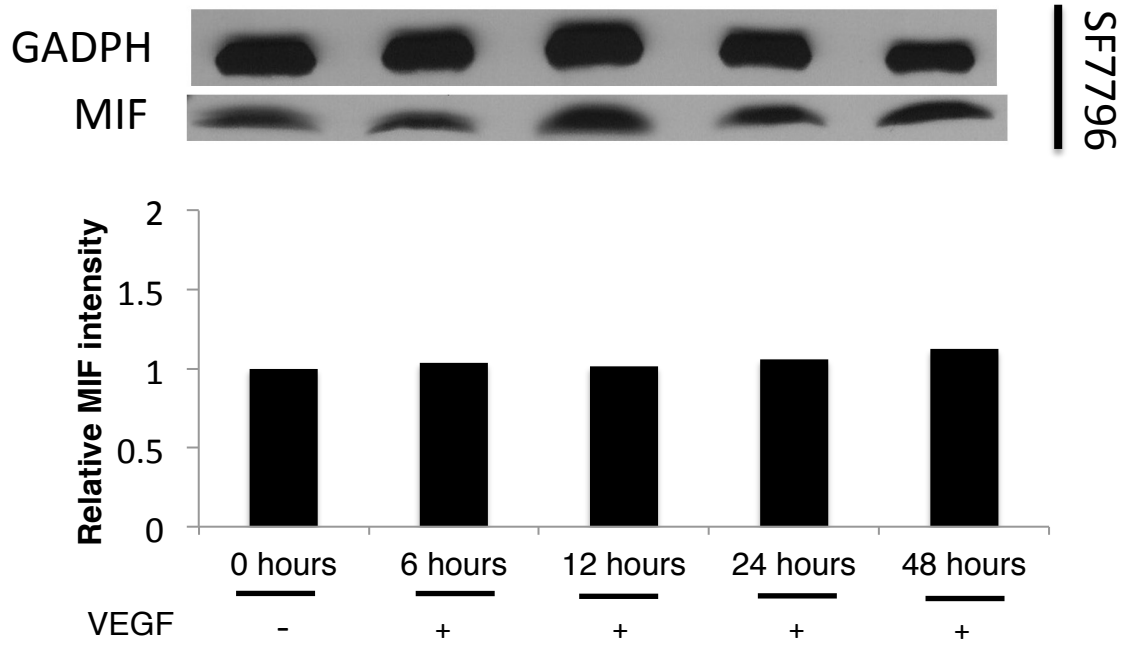

Supplementary Figure S13: VEGF stimulation of VEGFR2 low-expressing glioma cell line SF7796. No appreciable increase occurred in MIF expression when SF7796 cells were stimulated with 100 ng/mL rhVEGF.